HHS Public Access

Author manuscript

Nat Neurosci. Author manuscript; available in PMC 2012 March 01.

Published in final edited form as:

Nat Neurosci. ; 14(9): 1174–1181. doi:10.1038/nn.2894.

Hippocampal CA1 pyramidal cells form functionally distinct sublayers

Kenji Mizuseki, **Kamran Diba**, **Eva Pastalkova**, and **György Buzsáki**

Center for Molecular and Behavioral Neuroscience, Rutgers, The State University of New Jersey, 197 University Avenue, Newark, NJ 07102 New Jersey

Summary

Hippocampal CA1 pyramidal neurons have frequently been regarded as a homogeneous cell population in biophysical, pharmacological and modeling studies. Here we report robust differences between pyramidal neurons residing in the deep and superficial CA1 sublayers in the rat. Compared to their superficial peers, deep pyramidal cells fired at higher rates, burst more frequently, were more likely to have place fields and were more strongly modulated by slow oscillations of sleep. Both deep and superficial pyramidal cells fired preferentially at the trough of theta oscillations during maze exploration, yet during Rapid eye movement (REM) sleep, deep pyramidal cells shifted their preferred phase of firing to the peak of theta. Furthermore, whereas in waking, the majority of REM theta phase-shifting cells fired at the ascending phase of gamma oscillations, non-shifting cells preferred the trough. Thus, CA1 pyramidal cells in adjacent sublayers can address their targets jointly or differentially, depending on brain states.

Although the molecular, anatomical and functional diversity of cortical interneurons is well documented[1–3], principal cells are typically grouped together on the basis of their cortical layer and/or subregion assignments. However, several recent observations point to the existence of distinct subgroups of principal neurons with different properties, projections and local interactions, even within the same region and cortical layer[4–14]. In the neocortex and entorhinal cortex, specialized subnetworks of excitatory neurons have been described within[8–10] and across cortical layers[12,13]. These subnetworks may assist in segregating different streams of information[4,10,14].

The hippocampal CA1 region is a frequently used model system to study plasticity, pharmacological effects and intracellular features. In the rodent, CA1 pyramidal neurons form a compact layer consisting of 5 to 8 superimposed rows of pyramidal neurons. Each

Correspondence: György Buzsáki, Center for Molecular and Behavioral Neuroscience, Rutgers University, 197 University Avenue, Newark, NJ 07102, Tel: (973) 353-1080 ext. 3131, Fax: (973) 353-1820, buzsaki@axon.rutgers.edu.
Present address: Janelia Farm Research Campus, HHMI, Ashburn, VA. (E.P.), Dept. of Psychology, PO Box 413, University of Wisconsin at Milwaukee, Milwaukee, WI 53201 (K.D.)

AUTHOR CONTRIBUTIONS

K.M and G.B. designed the experiments. K.M., K.D., E.P. collected data, K.M. analyzed the data. K.M. and G.B. wrote the manuscript.

Note: Supplementary information is available on the Nature Neuroscience website.

pyramidal cell is typically assumed to have similar morphology, inputs, outputs and biophysical properties[15]. In contrast to this notion, anatomical experiments indicate that the medial and lateral entorhinal cortex project preferentially to proximal and distal parts of the CA1 region[16], respectively. Correlated with this topography, pyramidal cells show a gradually increasing propensity of emitting spike bursts[17] and decreasing spatial specificity in the proximo-distal (CA3-subicular) direction[18]. Other physiological observations also point to functional segregation in CA1 pyramidal cells. For example, the magnitude of somatodendritic backpropagation of action potential shows a bimodality, perhaps due to subtle morphological differences of pyramidal cells[19]. The phase preference of CA1 pyramidal cells to gamma oscillations also has a bimodal distribution[20].

Another potential source of variability of CA1 pyramidal neurons is the position or depth relative to the cell layer[21]. Supporting this hypothesis, early studies have demonstrated segregation of calbindin immunoreactivity[22] and zinc content[23] in the deep and superficial sub-strata of CA1 pyramidal layer and, more recently, striking within-layer differences have become apparent in gene expression studies[24,25]. Yet, functional differences between deep and superficial CA1 pyramidal neurons are not known, and most physiological experiments and modeling studies assume that pyramidal neurons in the CA1 sublayers are homogeneous. Exploiting the capability of silicon probes to localize the relative vertical position of neuronal somata in the recorded volume of neuronal tissue[26], we examined the functional properties of the superficial and deep CA1 pyramidal cells in the behaving rat. We describe two subcircuits, which are differentially controlled by intra- and extra-hippocampal inputs and can distinctly impact their targets in a brain-state dependent manner.

Results

Local field potentials (LFP) and unit firing were recorded in the hippocampal CA1 pyramidal layer (n = 10 rats; Fig. 1). In 4 of the animals, recordings were made simultaneously in CA1 and in multiple layers of the medial entorhinal cortex[27]. Recordings were carried out while the animal ran on an open field (180 cm by 180 cm, or 120 cm by 120 cm), a linear track (250 cm long), an elevated plus maze (100 cm by 100 cm), a zigzag maze (100 cm by 200 cm), or performed a T-maze alternation task or a rewarded wheel-running task[27] (hereafter theta periods during behavioral tasks are referred to as ‘RUN’). Recordings were also carried out during sleep, typically both before and after tasks, in the animal’s home cage.

Localization of neuronal somata in the CA1 pyramidal layer

The vertical span (140 μm) and the precise distribution of the 8 recording sites on the probe shanks (20 μm vertical steps) allowed for the determination of the relative depths of the cell bodies of the simultaneously recorded neurons (Fig. 1ac). The site with the largest spike amplitude for each unit was regarded as the location of the cell body[26] (Fig. 1d, arrows). The site with the largest amplitude of ripples, reflecting the middle of the pyramidal layer[28] (designated as site 0; Fig.1ac), was also determined for each shank (arrow in Fig. 1c) and served as the reference depth for calculating the distance of the cell bodies from the middle of the pyramidal layer.

Although the stratum oriens is stereotaxically above the pyramidal layer in the dorsal CA1 region of the rodent hippocampus, we follow the traditional terminology of cortical anatomy, where 'deep' and 'superficial' refer to direction of the basal and apical dendrites, respectively[29]. For reliably separating neurons according to depth, neurons with the largest action potentials at site 0 were termed 'middle', and those above (close to str. radiatum) and below (close to str. oriens) recording site 0 are referred to as 'superficial' and 'deep', respectively. The middle layer likely contained a mixture of deep and superficial neurons and served as a separator between the 'true' deep and superficial cells. These three tentative divisions contained approximately equal numbers of the recorded neurons (deep = 1,228, middle = 1,204 and superficial = 1,109). Somata above site 3 and below site 3 were rare (< 8.5 %) and were therefore lumped together with the somata recorded at sites 3 and 3, respectively.

Shifting theta phase preference between waking and REM

Five well-isolated[30] pyramidal neurons from a single shank were spatially distributed along the vertical (oriens-radiatum) axis (Fig. 1d). During maze exploration, all five of the neurons fired preferentially near the trough (180°) of the local field potential (LFP) theta recorded in the pyramidal layer. During REM sleep, the two superficial neurons continued to discharge near the trough, whereas the three neurons in the deeper parts of the layer shifted their preferred firing phase by almost half a theta cycle[31]. To quantify this observation across sessions and rats, the phase preference of each significantly theta phase-modulated pyramidal neuron was determined during both exploration and REM sleep. The preferred theta phase of neurons during REM sleep varied with depth ($P < 0.0001$; circular ANOVA), with deep neurons showing a preference for the peak of the theta waves, as shown by the significantly different mean theta phase preference of neurons at deeper sites (Fig. 2a; for individual rats, see Supplementary Fig. 1). To simplify further analysis, neurons recorded at different dephts were lumped into superficial, middle and deep subgroups. During REM sleep, the phase preference distributions across subgroups were significantly different (Fig. 2b; $P < 0.0001$; Watson's U^2-test; for individual rats, see Supplementary Fig. 1) but similar during RUN. In the deep sublayer in particular, approximately half of the pyramidal cells fired preferentially near the peak of theta during REM sleep.

RUN-REM phase shift-based classification—Since theta peak-preferring cells during REM may themselves comprise a functionally separate group that does not segregate perfectly in depth (Fig. 2b), we also separately compared the properties of REM phase-shifting and non-shifting cells, exploiting the bimodal distribution of phase preferences during REM (Fig. 2b and c). Pyramidal cells which were significantly phase-locked to theta oscillations during REM sleep (68.3 %, 1937 of 2838 CA1 pyramidal neurons which fired at least 50 spikes during REM), were broadly divided into 'REM-shifting' (< 120° or > 300° preferred theta phases during REM) and 'non-shifting' groups (120° to 300° preferred theta phases; Fig. 2c). Overall, 35.1 % (679 cells) belonged to the REM-shifting category. As expected, the depth distributions of REM-shifting and non-shifting neurons were significantly different (Fig. 2d; $P < 0.0001$, two-sample Kolmogorov-Smirnov test, one-tail). The ratio of REM-shifting cells doubled from the superficial-mid sublayers to the deep sublayer (Fig. 2d).

To compare these observations with CA1 interneurons and with neurons in the entorhinal cortex, the fraction of these cells which shifted their preferred phase from RUN to REM by more than 90° were calculated (Fig. 2e). In contrast to CA1 pyramidal cells, CA1 interneurons did not shift their preferred phase between wake and REM states. Furthermore, neurons with > 90° phase shift between RUN and REM in the various layers of the entorhinal cortex (EC2, EC3, EC5) were rare (Fig. 2e; Supplementary Fig. 2). Therefore, the theta phase shift of CA1 pyramidal neurons during REM sleep cannot simply be explained by altered timing from the entorhinal input (Supplementary Figs. 2 and 3).

Phase-locking of CA1 pyramidal cells by slow oscillations

To examine whether the CA1 sublayer-specific groups differed in other behavioral states, we examined their firing patterns during non-REM sleep as well. A prominent physiological feature of non-REM sleep in neocortical-paleocortical structures is the presence of slow cortical oscillations, associated with UP and DOWN states of neurons[32]. Slow oscillations also affect hippocampal network patterns[33]. To detect slow oscillations, the spiking activity of all simultaneously recorded EC neurons were summed and > 150 msec silent periods, followed by > 200 msec of activity were identified as DOWN-UP transitions[33] (Fig. 3, bottom). When segregated according to depth, neurons in superficial, middle and deep CA1 subgroups showed signficantly different magnitudes of modulation by the entorhinal slow oscillation (Fig. 3, top; $P < 0.0001$, $F = 22.19$; ANOVA; results in individual rats are shown in Supplementary Fig. 4).

RUN-REM phase shift-based classification—When segregated based on theta-phase shift during REM sleep, neurons in the REM-shifting group, relative to the non-shifting group, showed significantly stronger phase modulation by the slow oscillation (Fig. 3, middle; $P < 0.0001$; t-test). Together, these findings indicate that the entorhinal input can differentially activate superficial and deep subgroups of CA1 pyramidal cells during slow wave sleep.

We also investigated the relationship between sharp wave-ripple patterns[28] and the depth of CA1 pyramidal cells. The fraction of spikes during ripples (relative to all spikes during slow wave sleep episodes) was not significantly different between superficial and deep neurons (superficial = 8.17 ± 5.33 %, deep = 8.20 ± 4.95 %; $P > 0.2$, paired t-test, but the middle group was significantly higher than both sublayers; middle = 8.90 ± 4.93, mean ± S.D.). On the other hand, REM-shifting cells were more strongly associated with ripple activity as evidenced by both the higher fraction of spikes during ripples (8.94 ± 4.93 % vs 7.18 ± 4.12 %, $P<0.0001$; t-test) and a higher percentage of ripples associated with spiking (17.2 ± 12.1 % vs 15.4 ± 12.8 %, mean ± S.D., $P < 0.005$), relative to non-shifting cells. These findings indicate that REM-shifting neurons respond more vigorously to CA3 inputs during sharp wave-ripples.

Firing rate, burst and activity-dependence of theta phase

Next, we examined whether CA1 pyramidal cells in the different sublayers differ in their spiking properties and how these differences might relate to their theta phase preference. Neurons in the deeper part of the pyramidal layer had significantly higher overall firing rates

than did superficial neurons (Fig. 4a; P < 0.0001; see also Supplementary Fig. 5). In addition to rate, calulation of spike-burst index, defined as the fraction of spikes with < 6 ms interspike intervals[27,30], revealed that superficial neurons were significantly less 'bursty' than their deeper peers (Fig. 4b; P< 0.0001; Supplementary Fig. 6).

RUN-REM phase shift-based classification—Firing rate and burst propensities were also significantly different between REM-shifting and non-shifting cells (Supplementary Figs. 5 and 6). REM-shifting cells decreased their firing rates significantly more during REM sleep compared to RUN (Fig. 4c; P < 0.0001, t-test), and were also significantly more 'bursty' during REM sleep compared to RUN (Fig. 4d; P < 0.0001, t-test).

Because of the known correlation between discharge frequency and the theta phase of spikes[27,34,35], we examined how firing pattern changes, from single spikes to burst firing, affected the theta phase of spiking. Spikes of each neuron were sorted to eight interspike interval (ISI) categories, and the preferred theta phase and modulation depth were calculated for each neuron in each category[27] (Fig. 5; Supplementary Fig. 7, see Methods). During RUN, both REM-shifting and non-shifting neurons preferred the phase near the trough, with mostly a weak dependence on the ISI. An exception was for < 6 msec bursts in REM-shifting neurons, which showed a relatively wide phase preference (Fig. 5a and c). In contrast, during REM sleep, nearly all bursts of REM-shifting neurons preferred the peak of the theta cycle (Fig. 5b; < 15 msec interspike interval groups; P<0.0001, Watson-Williams test, RUN-REM comparison; Supplementary Fig. 7), whereas most single spikes (> 20 msec interspike intervals) continued to fire after the trough. In the non-shifting group both single spikes and bursts continued to fire after the trough during REM sleep (Fig. 5d).

During RUN, a large percentage of both REM-shifting and non-shifting neurons were significantly phase-modulated by theta, relatively independently of the inter-spike intervals (Fig. 5e). However, the percent of significantly theta-modulated neurons was larger for both bursts (ISI < 10 msec) and single spikes (ISI > 30 msec) in the REM-shifting group, compared with non-shifting cells. During REM sleep, the percent of significantly theta-modulated neurons during bursting was significantly higher in the REM-shifting than in the non-shifting group (P < 0.0001; chi-square independent test), whereas the percent of significantly theta-modulated neurons for single spikes was significantly higher in the non-shifting group compared to the REM-shifting group (P < 0.0001; Fig. 5f).

Within the significantly phase-modulated groups, we also analyzed the magnitude of theta phase-modulation ('mean resultant length'). Brain state change exerted a differential effect on the magnitude of theta phase-locking of spikes across the REM-shifting and non-shifting neurons (Fig. 5e and f). During RUN, non-shifting neurons were more strongly phase-locked than were REM-shifting cells, during both bursts (ISI < 10msec) and single spike firing (ISI > 30msec) patterns (Fig. 5e). During REM, this difference remained the same for single spikes but reversed for bursts. In fact, the theta phase-modulation of burst events (< 10 ms intervals) in REM-shifting neurons was almost twice as powerful during REM than during RUN (Fig. 5e and f). Comparison of ISI groups from REM-shifting neurons revealed that the same cells shifted their preferred phase from trough (ISI > 30 msec) to peak (ISI < 10 msec), and increased their phase modulation during burst events (Fig. 5g and h).

In summary, deep and superficial neurons have different firing rates and bursting properties. During REM sleep, REM-shifting (i.e., mainly deep) neurons burst more, compared to RUN, and bursts of spikes of REM-shifting cells are more strongly modulated by theta and show stronger theta peak preference, compared to non-shifting neurons. Thus, the interactions among instantaneous firing rate, bursting, theta modulation and preferred theta phase depend on the joint effect of brain state and cell location within the CA1 pyramidal layer.

Higher incidence of place cells in the deep CA1 sublayer

Hippocampal neurons in rodents show location-selective firing[36]. Neurons with peak firing rates exceeding 2 Hz on the linear track or on the open field (see Online Methods) were defined as place cells[18]. The proportion of place cells was significantly higher in the deep sublayer than in the superficial layer (Fig. 6). This was also the case when we used criteria of spatial coherence > 0.7 to define place fields[37,38] (Supplementary Fig. 8).

The distributions of peak firing rates and within-field mean rates were also significantly different across the depth groups (Supplementary Fig. 9 and 10) , consistent with the overall rate difference described above. Information content[39–41] (both bits per spike and bits per second) was also significantly different across the CA1 sublayers and between REM-shifting and non-shifting cells (Supplementary Figs. 9 and 10), with information content per spike being higher in the superficial and non-shifting groups than in the deep and REM-shifting groups. Other examined features of place cells (place field size, spatial coherence[37], stability[41]) were not different across the groups (Supplementary Figs. 9 and 10). In addition, the slopes of phase precession[42] on the linear track were similar across depth groups (Supplementary Fig. 10).

RUN-REM phase shift-based classification—Consistent with the results of the depth analysis, the proportion of place cells was significantly higher in the REM-shifting group, compared to non-shifting neurons in both the linear track and the open field (Fig. 6; $P < 0.001$; $P < 0.001$, respectively; Chi-square independent test). On the other hand, the slopes of phase precession[42] on the linear track were similar between the REM-shifting and non-shifting groups (Supplementary Fig. 10).

In summary, while the proportion of active place cells in a given environment was higher in the deep (REM-shifting) group, the major spatial features and theta phase dynamics of place cells were not different across groups.

Relationship between theta and gamma phase preference

The hippocampus also displays prominent gamma oscillations[43–45], and it was recently reported that in the waking rat, spikes of pyramidal cells show phase preference to either the trough (gammaT neurons, 30–240°) or the rising phase of the gamma wave[20] (gammaR neurons, 0–30, or 240–360°). We confirmed this bimodal gamma phase distribution during RUN (Fig. 7a), and also show that during REM, virtually all significantly gamma-modulated pyramidal cells were phase-locked to the trough of gamma waves[20] (Fig. 7a and b). The preferred gamma phase during RUN showed a depth-dependent shift, with a preference of

deep cells for the rising phase of the gamma cycle (Supplementary Fig. 11), although this effect was less robust than the depth-dependent theta-phase preference during REM. On the other hand, the match between gammaR and REM-shifting and between gammaT and non-shifting cells, respectively, was strong (Fig. 7), particularly in the middle and deep neurons (Supplementary Fig. 11). During REM, significantly fewer pyramidal cells were significantly phase-locked to gamma oscillations (REM = 10.4% vs RUN = 26.7%; $P < 0.0001$; chi-square independent test) or modulated by both theta and gamma oscillations (REM = 7.2 % vs RUN = 21.8 %; $P < 0.0001$; compare Fig. 7b and c) than during RUN. Significantly fewer REM-shifting cells were gamma modulated during REM sleep than during RUN ($P < 0.0001$, Chi-square independent test), while a comparable fraction of non-shifting cells were gamma modulated and fired at the trough of gamma both during REM and RUN. (Fig. 7b and c). The few gammaR pyramidal cells, which were significantly gamma phase-locked in both REM and RUN states, shifted their phase preference to the trough during REM (Supplementary Fig. 12). In contrast, putative CA1 interneurons maintained their gamma phase preference across behavioral states[20] (Supplementary Fig. 13).

Novelty does not affect theta phase preference during REM

Finally, the theta phase preference of pyramidal cells during REM sleep episodes both prior to and after exploration of a novel (n = 9 sessions in 4 rats) or familiar environment (n = 60 sessions) was compared. We examined whether the wake-REM shift in theta phase preference of CA1 pyramidal cell spikes was experience-dependent, since a previous study[31] suggested that after exposure to a novel arm of the maze, the phase preference of novel place field cells remains the same as observed during RUN, whereas REM sleep-related shift of phase preference emerges only after multiple experiences. In our experiments, for the majority of CA1 pyramidal cells (i.e., non-shifting cells), the preferred theta phase during REM remained similar during RUN, even after the familiar task (Fig. 8ac). Further, the distributions of theta phase difference between RUN and REM, tested after RUN sessions, were similar regardless of the familiarity of the task (Fig. 8ac, $P > 0.2$, Watson U^2 test), suggesting that environmental novelty did not significantly affect preferred theta phase of spiking during REM sleep.

In support of this observation, the preferred theta phases of the same neurons during REM sleep episodes before and after tasks were similar regardless of whether the task was novel or familiar (Fig. 8df).

Discussion

We found subpopulations of pyramidal cells with distinct responses to inputs, spiking properties and output influence, segregated in the superficial and deep parts of CA1 stratum pyramidale. Neurons residing in different sublayers differed in multiple properties, including theta phase preference and phase-modulation strength during REM sleep, modulation by slow oscillations and sharp-wave ripples during non-REM sleep, gamma phase preference during waking state, firing rate, bursting propensity and the proportion of cells with place fields. Although the CA1 pyramidal cells have often been tacitly assumed to be a

homogeneous population[15], the within-layer segregation of functional groups we found is in accord with the relatively distinct strata of superficial and deep pyramidal cells, first described by Lorente de Nó[29].

The stratification of function in the CA1 pyramidal layer is supported by a number of anatomical and molecular observations. Several surface and channel genes show sublayer-specific expression within the pyramidal layer[24,25]. In particular, both zinc and calbindin-containing pyramidal cells reside predominantly in the superficial layer (nearly all calbindin-immunoreactive neurons in this sublayer are zinc-positive[23]). Zinc amplifies AMPA receptor-mediated currents, and suppresses NMDA receptor-mediated responses[46]. Additionally, the Ca^{2+} buffer calbindin may play a role in synaptic plasticity, since long-term potentiation of Schaffer collateral synapses onto CA1 neurons and spatial learning are impaired in antisense transgenic calbindin-deficient mice[47]. In further support, the neurogenesis in the superficial layer occurs one to two days later during development than it does in the deep pyramidal cell layer[22]. Indeed, distinct subpopulations of principal neurons in each subfield (dentate gyrus, CA3 and CA1) of the hippocampus share gene expressions, distinct time windows of neurogenesis and synaptogenesis, and may form selective subcircuits[14]. Finally, neurons that project to the lateral septum are found largely in the deep CA1 sublayer[48], suggesting an output segregation of the distinct sublayers described here.

The robust correlation between the position of cells in the CA1 pyramidal layer and their physiological features may have multiple explanations. The simplest account is that intrinsic properties of pyramidal cells (morphology, distribution of ion-channels, receptors, etc) are responsible for most of the observed differences between sublayers. For example, morphological differences between the deep and superficial neurons[21,29] may differentially affect the bursting, firing rate and other biophysical properties of neurons, as described in the neocortex[6,7] and the CA3 region[49]. In turn, these intrinsic features would induce the different firing patterns and phase preferences observed during various LFP patterns, even if all neurons are uniformly innervated by afferents and local interneurons. In support of this possibility, we found reliable differences in firing rates and the bursting propensities of neurons in different sublayers. During REM sleep, bursts of REM-shifting (deep) cells (< 15 msec interspike intervals) displayed a stronger theta phase coupling than single spikes (> 20 msec), and bursts and single spikes preferred opposite phases of the theta cycle.

Another possible explanation is that deep and superficial neurons are targeted by differential sets of afferents and the observed changes simply reflect the distinct influence of their upstream partners. Supporting this hypothesis, deep CA1 neurons were more effectively entrained by slow oscillation of non-REM sleep, a potential indication that these (REM-shifting) neurons are more strongly driven by the entorhinal input. During theta oscillations, the CA1 region is under the competing influences of CA3 and entorhinal inputs. Again, the observed shifts of theta phase preferences of deep CA1 neurons can be explained by a stronger influence of the direct entorhinal input on these cells, given that during REM sleep EC3 principal neurons fired 10–25 msec before the REM-shifting CA1 neurons (Supplementary Figs. 3 and 14). Most likely, circuit and intrinsic properties interact with each other during ontogenesis so that the spatial position of neurons may correlate with both their integration into the circuitry and their intrinsic properties[12,14].

Neither intrinsic nor circuit properties alone can adequately explain the two distinct cell groups, REM-shifting and non-shifting cells, because physiological features defining the two groups are brain-state dependent. A fundamental difference between the waking state and REM sleep is the dramatically reduced tonic release of several subcortical neurotransmitters, including serotonin, norepinephrine and histamine, during REM sleep[50]. Subcortical neuromodulators may distinctly affect the REM-shifting and non-shifting cells, by changing differentially both their intrinsic properties and their synaptic interactions in the network in which they are embedded, thereby producing significantly distinct changes in firing rates, bursting propensity and theta phase of spiking.

In summary, functionally distinct sublayers are present in the CA1 hippocampal region. These may serve different functions, such as melding streams of information or segregating them, depending on brain state. In the waking animal, the inputs may be integrated by the co-firing of superficial and deep neurons at the theta trough and streamlined to their joint targets. In contrast, during REM sleep the different inputs may be kept separate or perhaps the same inputs may address both deep and superficial neurons but can then be routed to different targets and/or at different phases of the theta cycle. Although they represent a minority, the REM-shifting deep neurons fire bursts of spikes on the peak of theta during REM sleep and, therefore, may exert as powerful a downstream effect as the non-shifting, trough-preferring majority. The behavioral significance of such brain-state dependent integration and segregation of neuronal information by the CA1 region remains to be explored.

METHODS

Methods and any associated references are available in the online version of the paper at http://www.nature.com/natureneuroscience/

Supplementary Material

Refer to Web version on PubMed Central for supplementary material.

Acknowledgments

We thank E. Cela, S. Fujisawa, P.M. Hiche, S. Ozen, A. Sirota, E. Stark and Y. Wang for comments on the manuscript, and D. Sullivan for valuable suggestions. Supported by National Institutes of Health (NS034994; MH54671), National Science Foundation, the J.D. McDonnell Foundation, Uehara Memorial Foundation, Astellas Foundation for Research on Metabolic Disorders, the Japan Society of Promotion for Sciences and the Robert Leet & Clara Guthrie Patterson Trust.

References

1. Freund TF, Buzsaki G. Interneurons of the hippocampus. Hippocampus. 1996; 6:347–470. [PubMed: 8915675]
2. Markram H, et al. Interneurons of the neocortical inhibitory system. Nat Rev Neurosci. 2004; 5:793–807. [PubMed: 15378039]
3. Klausberger T, Somogyi P. Neuronal diversity and temporal dynamics: the unity of hippocampal circuit operations. Science. 2008; 321:53–57. [PubMed: 18599766]
4. Nelson SB, Sugino K, Hempel CM. The problem of neuronal cell types: a physiological genomics approach. Trends Neurosci. 2006; 29:339–345. [PubMed: 16714064]

5. Connors BW, Gutnick MJ, Prince DA. Electrophysiological properties of neocortical neurons in vitro. J Neurophysiol. 1982; 48:1302–1320. [PubMed: 6296328]
6. Chagnac-Amitai Y, Luhmann HJ, Prince DA. Burst generating and regular spiking layer 5 pyramidal neurons of rat neocortex have different morphological features. J Comp Neurol. 1990; 296:598–613. [PubMed: 2358553]
7. Mason A, Larkman A. Correlations between morphology and electrophysiology of pyramidal neurons in slices of rat visual cortex. II Electrophysiology. J Neurosci. 1990; 10:1415–1428. [PubMed: 2332788]
8. Song S, Sjostrom PJ, Reigl M, Nelson S, Chklovskii DB. Highly nonrandom features of synaptic connectivity in local cortical circuits. PLoS Biol. 2005; 3:e68. [PubMed: 15737062]
9. Yoshimura Y, Dantzker JL, Callaway EM. Excitatory cortical neurons form fine-scale functional networks. Nature. 2005; 433:868–873. [PubMed: 15729343]
10. Varga C, Lee SY, Soltesz I. Target-selective GABAergic control of entorhinal cortex output. Nat Neurosci. 2010; 13:822–824. [PubMed: 20512133]
11. Wang Y, et al. Heterogeneity in the pyramidal network of the medial prefrontal cortex. Nat Neurosci. 2006; 9:534–542. [PubMed: 16547512]
12. Yu YC, Bultje RS, Wang X, Shi SH. Specific synapses develop preferentially among sister excitatory neurons in the neocortex. Nature. 2009; 458:501–504. [PubMed: 19204731]
13. Thomson AM, West DC, Wang Y, Bannister AP. Synaptic connections and small circuits involving excitatory and inhibitory neurons in layers 2–5 of adult rat and cat neocortex: triple intracellular recordings and biocytin labelling in vitro. Cereb Cortex. 2002; 12:936–953. [PubMed: 12183393]
14. Deguchi Y, Donato F, Galimberti I, Cabuy E, Caroni P. Temporally matched subpopulations of selectively interconnected principal neurons in the hippocampus. Nat Neurosci. 2011; 14:495–504. [PubMed: 21358645]
15. Amaral, D.; Lavenex, P. Hippocampal Neuroanatomy. In: Andersen, P.; Morris, R.; Amaral, D.; Bliss, TVP.; O'Keefe, J., editors. The hippocampus book. Oxford University Press; 2007. p. 37-114.
16. Tamamaki N, Nojyo Y. Preservation of topography in the connections between the subiculum, field CA1, and the entorhinal cortex in rats. J Comp Neurol. 1995; 353:379–390. [PubMed: 7538515]
17. Jarsky T, Mady R, Kennedy B, Spruston N. Distribution of bursting neurons in the CA1 region and the subiculum of the rat hippocampus. J Comp Neurol. 2008; 506:535–547. [PubMed: 18067146]
18. Henriksen EJ, et al. Spatial representation along the proximodistal axis of CA1. Neuron. 2010; 68:127–137. [PubMed: 20920796]
19. Golding NL, Kath WL, Spruston N. Dichotomy of action-potential backpropagation in CA1 pyramidal neuron dendrites. J Neurophysiol. 2001; 86:2998–3010. [PubMed: 11731556]
20. Senior TJ, Huxter JR, Allen K, O'Neill J, Csicsvari J. Gamma oscillatory firing reveals distinct populations of pyramidal cells in the CA1 region of the hippocampus. J Neurosci. 2008; 28:2274–2286. [PubMed: 18305260]
21. Bannister NJ, Larkman AU. Dendritic morphology of CA1 pyramidal neurones from the rat hippocampus: I. Branching patterns. J Comp Neurol. 1995; 360:150–160. [PubMed: 7499560]
22. Baimbridge KG, Peet MJ, McLennan H, Church J. Bursting response to current-evoked depolarization in rat CA1 pyramidal neurons is correlated with lucifer yellow dye coupling but not with the presence of calbindin-D28k. Synapse. 1991; 7:269–277. [PubMed: 2042109]
23. Slomianka L. Neurons of origin of zinc-containing pathways and the distribution of zinc-containing boutons in the hippocampal region of the rat. Neuroscience. 1992; 48:325–352. [PubMed: 1376449]
24. Thompson CL, et al. Genomic anatomy of the hippocampus. Neuron. 2008; 60:1010–1021. [PubMed: 19109908]
25. Dong HW, Swanson LW, Chen L, Fanselow MS, Toga AW. Genomic-anatomic evidence for distinct functional domains in hippocampal field CA1. Proc Natl Acad Sci U S A. 2009; 106:11794–11799. [PubMed: 19561297]

26. Csicsvari J, et al. Massively parallel recording of unit and local field potentials with silicon-based electrodes. J Neurophysiol. 2003; 90:1314–1323. [PubMed: 12904510]
27. Mizuseki K, Sirota A, Pastalkova E, Buzsaki G. Theta oscillations provide temporal windows for local circuit computation in the entorhinal-hippocampal loop. Neuron. 2009; 64:267–280. [PubMed: 19874793]
28. Ylinen A, et al. Sharp wave-associated high-frequency oscillation (200 Hz) in the intact hippocampus: network and intracellular mechanisms. J Neurosci. 1995; 15:30–46. [PubMed: 7823136]
29. Lorente de Nó R. Studies on the structure of the cerebral cortex. II. Continuation of the study of the ammonic system. J Psychol Neurol (Lpz). 1934; 46:113–177.
30. Harris KD, Hirase H, Leinekugel X, Henze DA, Buzsaki G. Temporal interaction between single spikes and complex spike bursts in hippocampal pyramidal cells. Neuron. 2001; 32:141–149. [PubMed: 11604145]
31. Poe GR, Nitz DA, McNaughton BL, Barnes CA. Experience-dependent phase-reversal of hippocampal neuron firing during REM sleep. Brain Res. 2000; 855:176–180. [PubMed: 10650147]
32. Steriade M, Nunez A, Amzica F. A novel slow (< 1 Hz) oscillation of neocortical neurons in vivo: depolarizing and hyperpolarizing components. J Neurosci. 1993; 13:3252–3265. [PubMed: 8340806]
33. Isomura Y, et al. Integration and segregation of activity in entorhinal-hippocampal subregions by neocortical slow oscillations. Neuron. 2006; 52:871–882. [PubMed: 17145507]
34. Harris KD, et al. Spike train dynamics predicts theta-related phase precession in hippocampal pyramidal cells. Nature. 2002; 417:738–741. [PubMed: 12066184]
35. Mehta MR, Lee AK, Wilson MA. Role of experience and oscillations in transforming a rate code into a temporal code. Nature. 2002; 417:741–746. [PubMed: 12066185]
36. O'Keefe J, Dostrovsky J. The hippocampus as a spatial map. Preliminary evidence from unit activity in the freely-moving rat. Brain Res. 1971; 34:171–175. [PubMed: 5124915]
37. Muller RU, Kubie JL. The firing of hippocampal place cells predicts the future position of freely moving rats. J Neurosci. 1989; 9:4101–4110. [PubMed: 2592993]
38. Hafting T, Fyhn M, Bonnevie T, Moser MB, Moser EI. Hippocampus-independent phase precession in entorhinal grid cells. Nature. 2008; 453:1248–1252. [PubMed: 18480753]
39. Skaggs, WE.; McNaughton, BL.; Gothard, KM.; Markus, EJ. An information-theoretic approach to deciphering the hippocampal code. In: Hanson, SJ.; Cowan, JD.; Giles, CL., editors. Advances in neural information processing systems. Vol. 5. San Mateo, CA: Morgan Kaufmann; 1993. p. 1030-1037.
40. Skaggs WE, McNaughton BL, Wilson MA, Barnes CA. Theta phase precession in hippocampal neuronal populations and the compression of temporal sequences. Hippocampus. 1996; 6:149–172. [PubMed: 8797016]
41. Markus EJ, Barnes CA, McNaughton BL, Gladden VL, Skaggs WE. Spatial information content and reliability of hippocampal CA1 neurons: effects of visual input. Hippocampus. 1994; 4:410–421. [PubMed: 7874233]
42. O'Keefe J, Recce ML. Phase relationship between hippocampal place units and the EEG theta rhythm. Hippocampus. 1993; 3:317–330. [PubMed: 8353611]
43. Bragin A, et al. Gamma (40–100 Hz) oscillation in the hippocampus of the behaving rat. J Neurosci. 1995; 15:47–60. [PubMed: 7823151]
44. Whittington MA, Traub RD, Jefferys JG. Synchronized oscillations in interneuron networks driven by metabotropic glutamate receptor activation. Nature. 1995; 373:612–615. [PubMed: 7854418]
45. Csicsvari J, Jamieson B, Wise KD, Buzsaki G. Mechanisms of gamma oscillations in the hippocampus of the behaving rat. Neuron. 2003; 37:311–322. [PubMed: 12546825]
46. Peters S, Koh J, Choi DW. Zinc selectively blocks the action of N-methyl-D-aspartate on cortical neurons. Science. 1987; 236:589–593. [PubMed: 2883728]
47. Molinari S, et al. Deficits in memory and hippocampal long-term potentiation in mice with reduced calbindin D28K expression. Proc Natl Acad Sci U S A. 1996; 93:8028–8033. [PubMed: 8755597]

48. Sorensen JC, Tonder N, Slomianka L. Zinc-positive afferents to the rat septum originate from distinct subpopulations of zinc-containing neurons in the hippocampal areas and layers. A combined fluoro-gold tracing and histochemical study. Anat Embryol (Berl). 1993; 188:107–115. [PubMed: 8214627]

49. Bilkey DK, Schwartzkroin PA. Variation in electrophysiology and morphology of hippocampal CA3 pyramidal cells. Brain Res. 1990; 514:77–83. [PubMed: 2357533]

50. Pace-Schott EF, Hobson JA. The neurobiology of sleep: genetics, cellular physiology and subcortical networks. Nat Rev Neurosci. 2002; 3:591–605. [PubMed: 12154361]

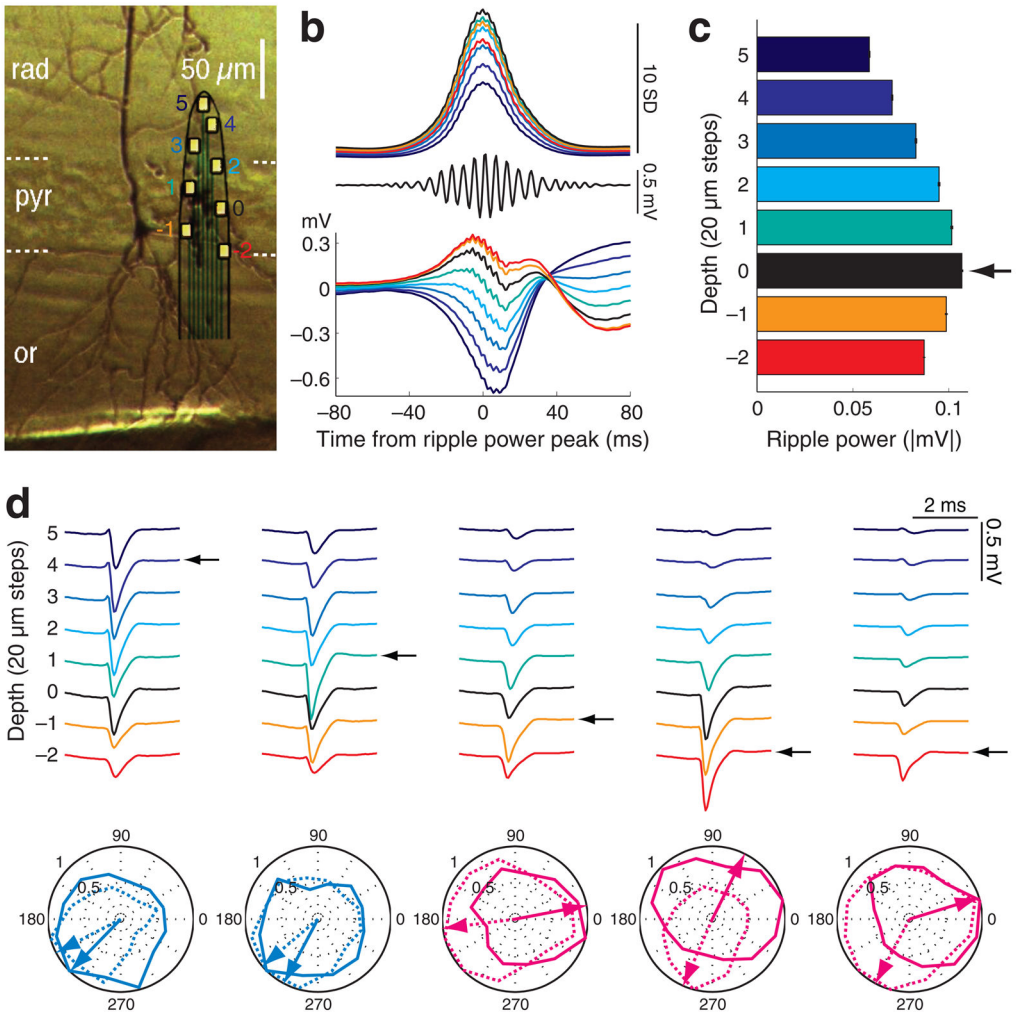

Figure 1. Spatial localization of neuronal somata in the CA1 pyramidal layer

a, Biocytin-filled neuron in the deep CA1 pyramidal cell layer. Surrounding unstained neuronal somata provide reference for the recording sites of the superposed silicon probe. Color-coded recording sites (2 to 5) are the same in parts **b** to **d**. 0, designates the middle of the layer, determined by the maximum ripple power (black in **b d**). **b d**, data from a shank from a single session. **b**, Middle, filtered (140–230 Hz) single trace at depth 0. Bottom, average LFP traces triggered by ripple power peaks (n = 2,635), recorded at different depths. Top, mean integrated ripple power at different depths, normalized by the standard deviation of ripple power at depth 0. **c**, Ripple power at different recording depths (mean ± S.E.M., from part **b**, top). The recording site with the largest ripple power identifies the middle of the pyramidal layer (arrow, reference depth 0), and serves for the determination of the distance of the recorded cell body of individual neurons from the middle of the layer. **d**, Average waveforms of 5 simultaneously recorded neurons (1Hz–5 kHz). Arrows indicate the putative position of the neuron's soma relative to the reference depth, inferred from the largest spike amplitude[26]. Two 'superficial' neurons (i.e., above reference depth 0) and three 'deep' neurons (below reference depth 0) are shown. Polar plots of spike phase distribution of the 5 neurons referenced to the theta oscillation in the CA1 pyramidal layer (peak of theta

= 0, 360 °, trough = 180 °). Normalized contour plots and preferred spike phase of the neurons (arrows) during maze running (dotted) and REM sleep (solid). Magenta polar plots represent REM-shifting neurons and light blue plots non-shifting cells. Positive polarity is up in all figures.

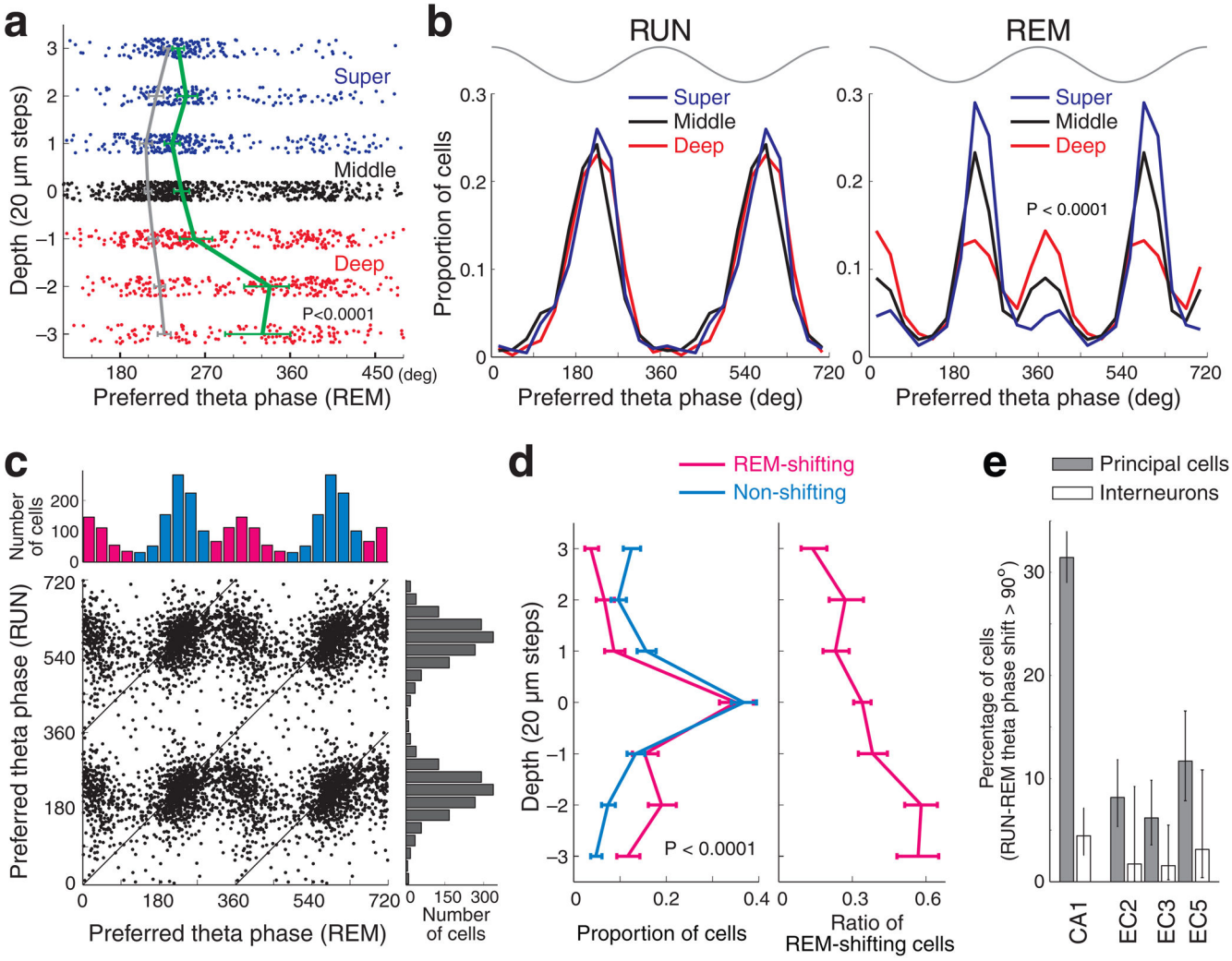

Figure 2. Preferred theta phase of spikes during REM sleep depends on the position of the soma in the CA1 pyramidal layer

a, Preferred theta phase for each neuron (dots) recorded at different depths of the layer during REM sleep. Solid lines; mean (± 95% confidence intervals) preferred theta phase (green, REM). For comparison, the mean preferred theta phase during RUN (gray) is also shown. The few neurons above and below recording sites 3 and 3 were added to values at 3 and 3, respectively. **b,** Distribution of the preferred theta phase of pyramidal cells in the superficial (recording sites above 0), middle (site 0) and deep (sites below 0) depths during maze running (RUN) and REM sleep. Note unimodal distribution of theta phase preference in the deep layer group during RUN and bimodal distribution during REM sleep. Top gray traces, idealized reference theta cycle in CA1 pyramidal layer. **c,** Distribution of preferred theta phases during RUN and REM sleep. Only neurons which showed significant theta phase modulation during both RUN and REM sleep are included here. Top and right: theta phase preference histograms for REM sleep and RUN. Note bimodal distribution of preferred theta phase during REM sleep. Neurons with < 120° or > 300° preferred theta phases during REM (magenta) were designated as REM-shifting cells, while those between 120° to 300° (light blue) as non-shifting cells. **d**, Left, depth distribution of REM-shifting

and non-shifting neurons (± 95% Clopper-Pearson confidence intervals). Right, distribution of the fraction of REM-shifting cells as a function of depth in the pyramidal layer. **e**, Percent of neurons with > 90° phase shift between RUN and REM (± 95% Clopper-Pearson confidence intervals) in different regions. EC2, EC3, EC5 correspond to neurons in layers II, III and V of the entorhinal cortex, respectively. Interneurons did not shift phase preference across states. Theta phase of LFP recorded from the CA1 pyramidal cell layer was used for all the cell types.

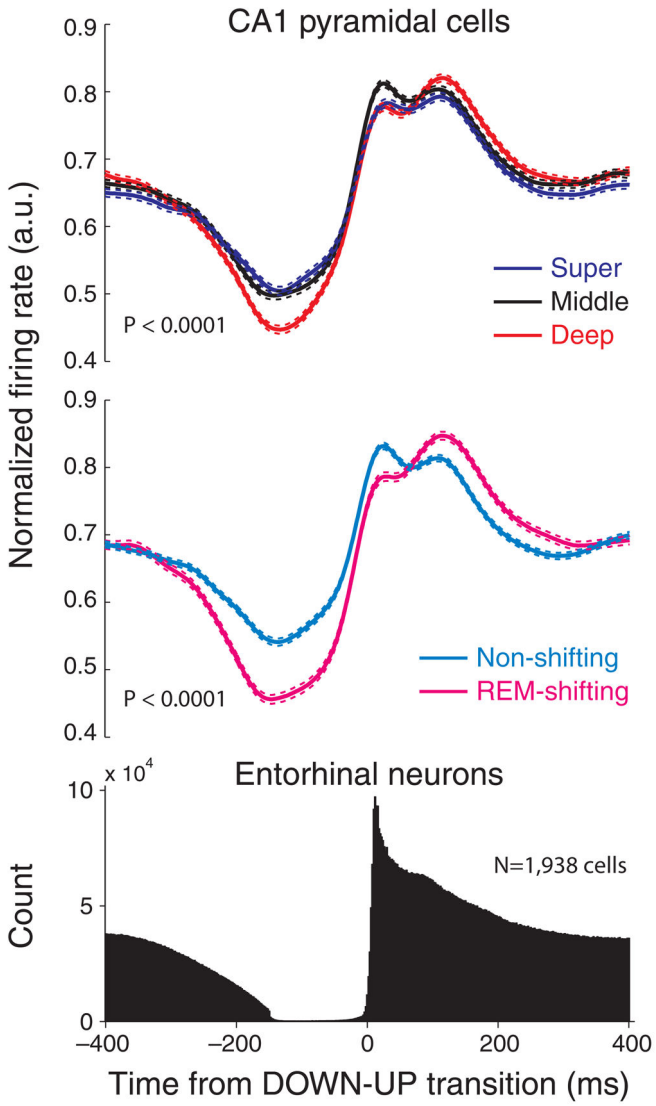

Figure 3. Phase-locking of CA1 pyramidal cell spikes by slow oscillations is location-dependent

Top, peri-event firing rate histograms of CA1 pyramidal neurons in the superficial (super), middle and deep sublayers during slow oscillations in sleep. Firing rates of single cells were normalized by peak firing rates. Mean ± S.E.M. is shown for each group. Middle, rate histograms of REM-shifting and non-shifting neurons. Bottom, entorhinal cortex unit firing histogram. Time zero: DOWN-UP transition of slow oscillation.

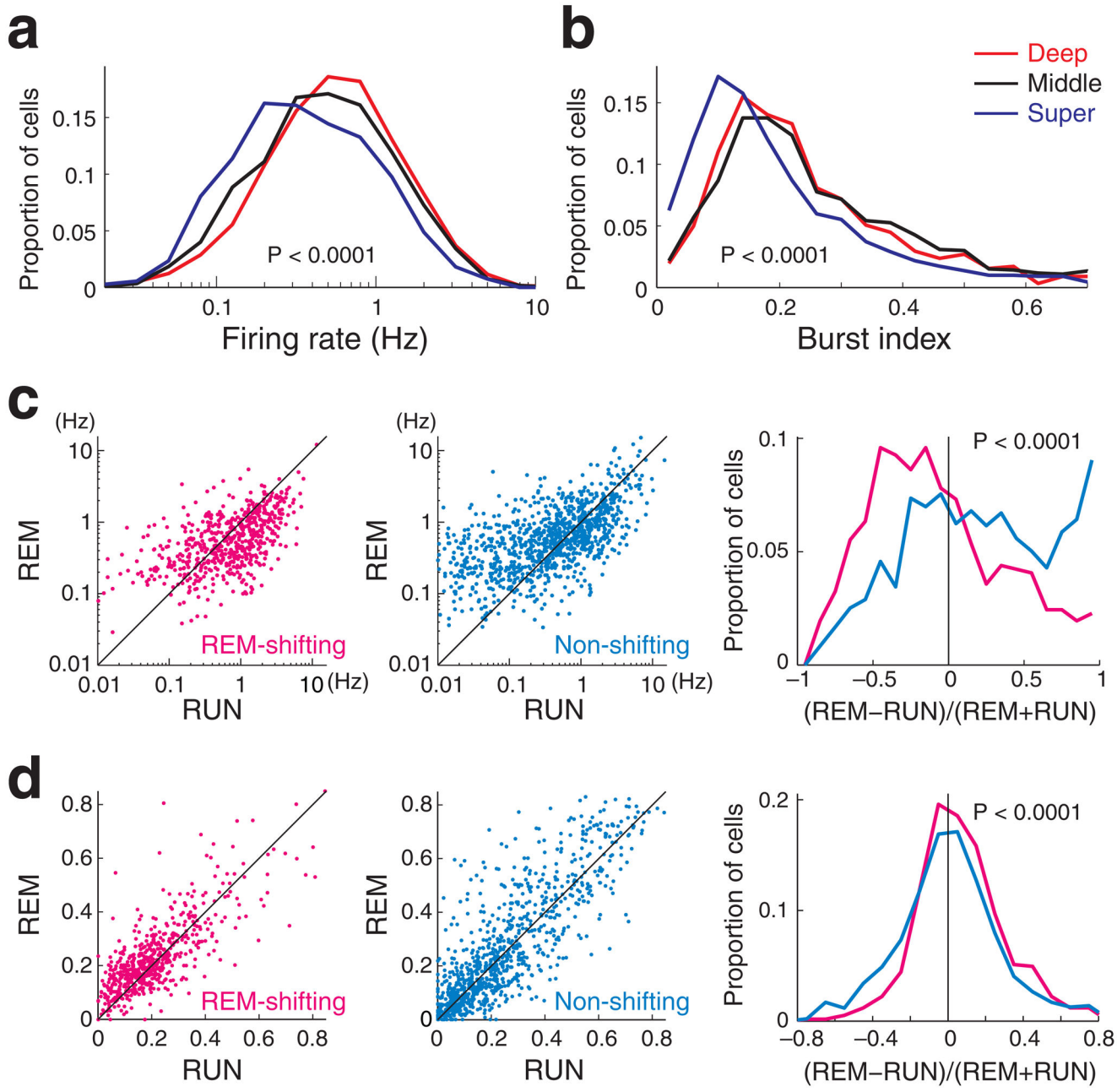

Figure 4. Firing rates and bursting properties of CA1 pyramidal cells

(a) Distribution of overall firing rates (Hz, log scale) and (**b)** burst index (fraction of spikes with < 6 msec interspike intervals, either preceding or following spikes) for neurons located in the superficial, middle and deep sublayers. **c,** Firing rates of REM-shifting (left) and non-shifting neurons (middle) during maze running (RUN) and REM sleep. REM-shifting neurons were significantly less active during REM sleep than during RUN. Right panel, distribution of the magnitude and direction of firing rate changes across states. **d,** Burst index of REM-shifting and non-shifting neurons during maze running (RUN) and REM

sleep. REM-shifting neurons were significantly more bursty during REM sleep than during RUN.

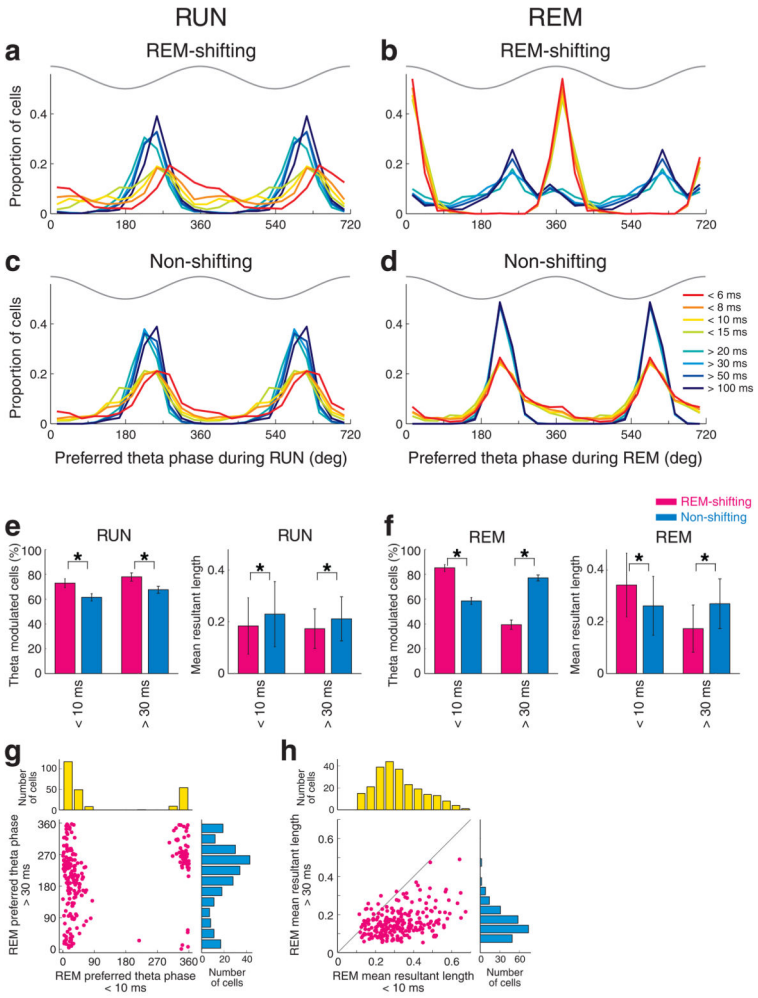

Figure 5. Interspike interval-theta phase relationship of CA1 pyramidal cells

a–d, Distribution of the preferred theta phase of REM-shifting and non-shifting neurons in each interspike interval category. Note the different theta phase preference during RUN (**a**) and abrupt theta phase shift during REM sleep (**b**) in REM-shifting neurons in relation with the changes of interspike intervals from < 15 msec to > 20 msec. Theta phase preference of non-shifting neurons (**c, d**) was less sensitive to changes in interspike intervals. Top gray traces, idealized reference theta cycle in CA1 pyramidal layer. **e**, Left, percent of significantly theta phase-modulated neurons (± 95% Clopper-Pearson confidence intervals) and the strength of theta phase-locking (mean resultant length, mean ± S.D.) in < 10 msec and > 30 msec interspike interval categories during RUN. REM-shifting (magenta) and non-shifting (light blue) neurons are shown separately. **f**, same for REM sleep. All comparisons between REM-shifting and non-shifting groups are significant (*, $P < 0.0001$, Chi-square test for percent of modulated cells; paired t-test for mean resultant length). **g**. Comparison of preferred theta phase between < 10 msec and > 30 msec categories of the same neurons during REM sleep. Only REM-shifting cells significantly modulated for both ISI categories are shown. **h**. Same as **g** but comparison of mean resultant length.

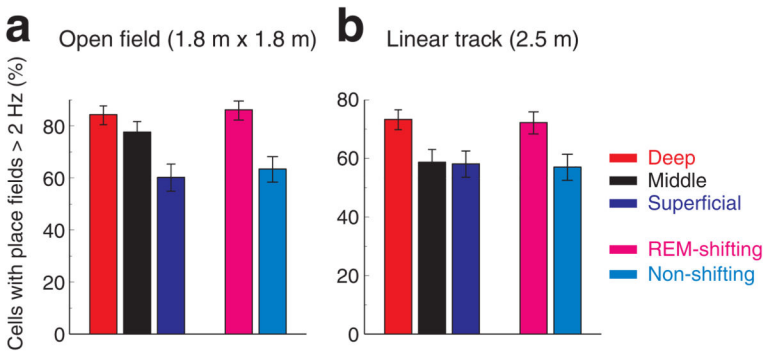

Figure 6. Larger fraction of place cells in deep layer neurons and REM-shifting group

a. Proportion of neurons with place fields, defined by peak firing rate (> 2 Hz; Online Methods), in different sublayers and in the REM-shifting and non-shifting groups during open field exploration. Clopper-Pearson confidence intervals ($P < 0.05$) are shown. **b**, Same for neurons recorded on the linear track. (For other spatial features, see Supplementary Figs. 8–10).

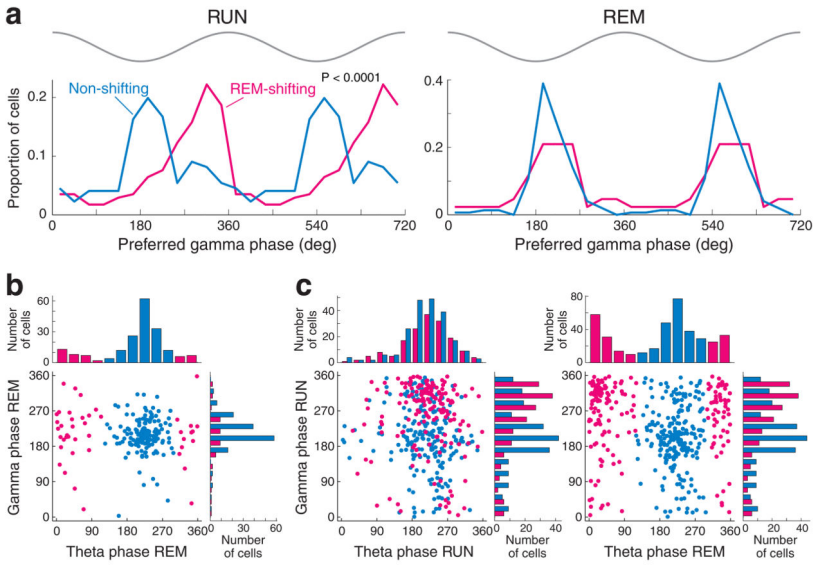

Figure 7. Relationship between theta and gamma phase-preferences of CA1 pyramidal cells

a, Distribution of preferred phase of gamma oscillation (30–80 Hz) during maze running (RUN) and REM sleep, shown separately for REM-shifting and non-shifting neurons. Note that both groups fired preferentially at the trough of local gamma waves (~180°) during REM sleep, whereas the majority of REM-shifting neurons were phase-locked to the rising phase (gammaR) of the gamma cycle during RUN. The reference site for LFP gamma was the middle of the pyramidal layer (site 0 in Fig. 1). Two gamma cycles are shown for better visibility. Top gray traces, idealized reference gamma cycle in CA1 pyramidal layer. **b, c,** Modulation of pyramidal cells by both gamma and theta. Note that most gamma-modulated neurons during REM are non-shifting neurons (**b,** light blue) and most gammaR neurons during RUN belong to the REM-shifting group (**c**, magenta). The side histograms in **b** and **c** (right) are the same as the plots in **a**. Only neurons, which were significantly modulated by both theta and gamma oscillations are included in the plots of **b** and **c**.

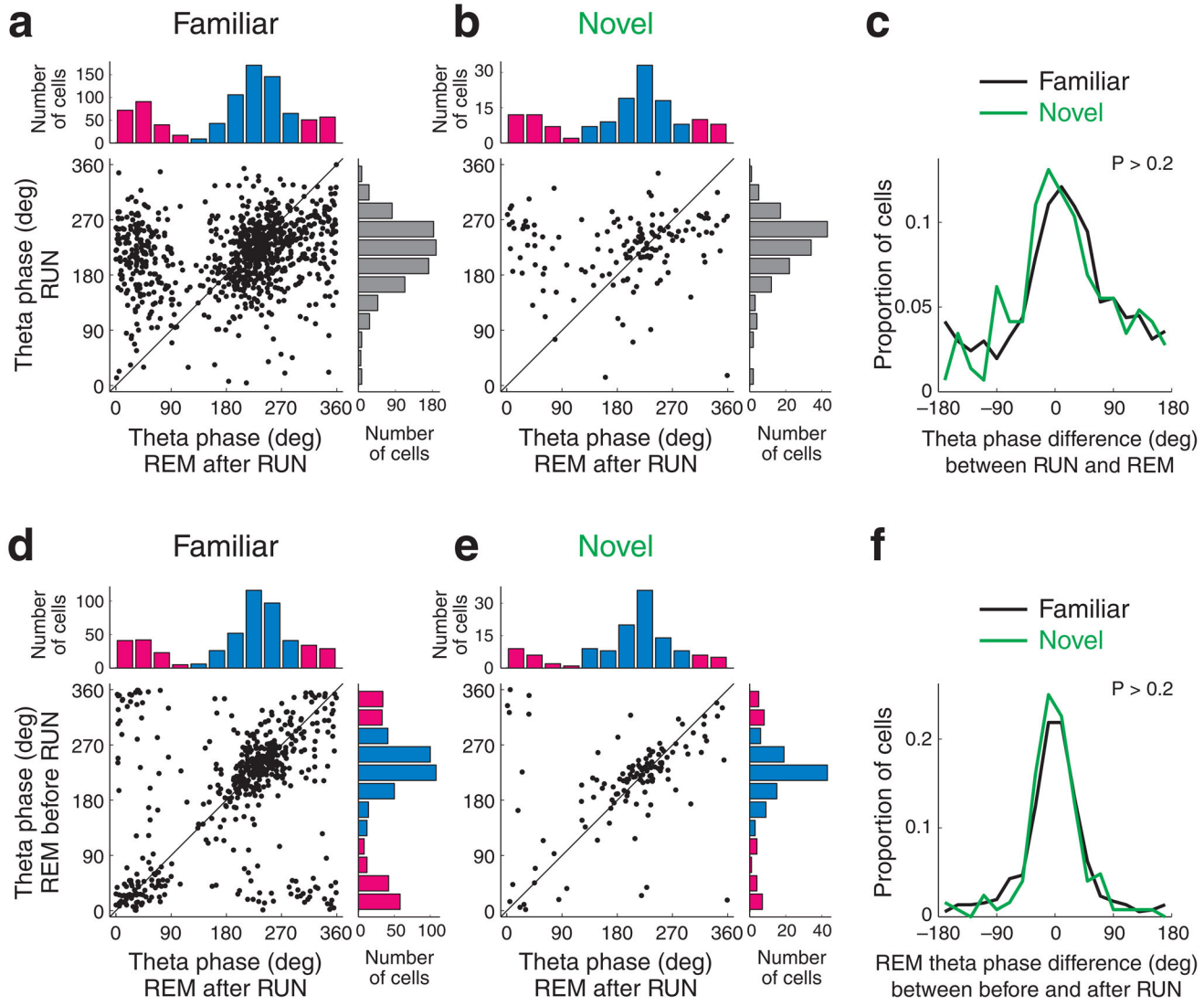

Figure 8. The theta phase of spikes during REM is not affected by novel experience

a, b. Relationship between preferred theta phase during RUN and REM after RUN sessions in familiar (**a**) and novel (**b**) tasks. **c**. Distribution of theta phase shifts between RUN and REM after RUN sessions. Familiar and novel tasks are shown separately. **d, e.** Preferred theta phase of CA1 pyramidal neurons during REM sleeps before and after a familiar task (**d**) and a novel task (**e**). **f**. Distribution of preferred theta phase differences between REM sleeps before and after task. Note similar phase preference, independent of task novelty (Watson U^2 test, $P > 0.2$).